



A Comparison of sector-scan and dual Doppler wind measurements at Høvsøre Test Station – one lidar or two?

Simon, Elliot; Courtney, Michael

Publication date:
2016

Document Version
Publisher's PDF, also known as Version of record

[Link back to DTU Orbit](#)

Citation (APA):
Simon, E., & Courtney, M. (2016). *A Comparison of sector-scan and dual Doppler wind measurements at Høvsøre Test Station – one lidar or two?* DTU Wind Energy. DTU Wind Energy E Vol. 0112

General rights

Copyright and moral rights for the publications made accessible in the public portal are retained by the authors and/or other copyright owners and it is a condition of accessing publications that users recognise and abide by the legal requirements associated with these rights.

- Users may download and print one copy of any publication from the public portal for the purpose of private study or research.
- You may not further distribute the material or use it for any profit-making activity or commercial gain
- You may freely distribute the URL identifying the publication in the public portal

If you believe that this document breaches copyright please contact us providing details, and we will remove access to the work immediately and investigate your claim.

A Comparison of sector-scan and dual Doppler wind measurements at Høvsøre Test Station – one lidar or two?

DTU Wind Energy Report E-0112

ISBN: 978-87-93278-69-1

Elliot I. Simon and Michael S. Courtney

Department of
Wind Energy
E Report 2016



Authors: Elliot I. Simon and Michael S. Courtney

Title: A Comparison of sector-scan and dual Doppler wind measurements at Høvsøre Test Station – one lidar or two?

Department: DTU Wind Energy, Risø Campus

Summary (max 2000 characters):

Long range scanning lidars have the ability to be deployed along the coastline to measure the near shore wind resource. Within the wind energy scope, this is most applicable to assessing the potential energy production (and thus revenue) of a prospected near shore wind farm (here defined as 3-12km from the coast). Ground based remote sensing has numerous advantages over traditional in-situ (offshore met mast) and buoy based installations, mainly in terms of cost, complexity, and failure/delay risk. Since each lidar can only measure a portion of the wind vector, it is necessary to either deploy two devices in tandem (dual Doppler) or employ a single Doppler scanning strategy such as PPI (plan position indicator, or sector scan) which allows for estimation of the two component horizontal wind vector. In preparation for a six month long measurement campaign along the Danish North Sea, a one week experiment was performed at DTU's test centre for large wind turbines (Høvsøre), which lies 1.8km inland and consists of flat terrain with predominate winds from offshore. Two lidars in staring dual Doppler mode and one lidar performing 60 degree sector scans had their beams collocated atop a 116.5m met-mast, which provided reference wind speed and direction values. The 10 minute reconstructed lidar measurements were in excellent agreement with the reference instrumentation. The dual Doppler results matched within 0.1% of the reference wind speed, with very low levels of unbiased scatter. Sector scan results also indicate very good agreement with the met-mast, corresponding within 0.2% for wind speed, with an R^2 of 0.998. The sector scan results for wind speed exhibit larger amounts of scatter than with dual Doppler, however the bias is centred around the regression line which gives good indication that wind measurements taken using the sector scan method are valid and acceptable for use in performing wind resource studies in simple terrain and in offshore conditions. Further, we show that when measuring in these cases, a sector size of 38 degrees still measures within 0.6% of the reference data for wind speed.

Project no.:

2015-1-12263

Sponsorship:

ForskEL

Pages: 36

References: 5

Danmarks Tekniske Universitet

DTU Vindenergi
Nils Koppels Allé
Bygning 403
2800 Kgs. Lyngby
Telephone

www.vindenergi.dtu.dk

Preface

This report encompasses deliverable D1.2 of the ForskEL project RUNE (Reducing uncertainty of near-shore wind resource estimates using onshore lidars). It is an abridged version of the master thesis work completed at DTU by Elliot I. Simon while enrolled at Uppsala University in Sweden. The full text is available at the following link: http://orbit.dtu.dk/files/125274101/Thesis_Elliot_DTU_final.pdf

DTU, Risø Campus, June 2016

Elliot I. Simon & Michael S. Courtney

Content

Summary	5
1. Introduction	6
1.1 The need for near-coastal wind data	6
1.2 Goal of this report	7
1.3 Structure of this report	7
2. Measuring wind speeds using scanning lidars	8
2.1 General remarks	8
2.2 Dual Doppler	8
2.3 Sector scanning (partial PPI)	9
3. The measurement campaign	11
3.1 Site description	11
3.2 The instrumentation	14
4. Methodology	16
4.1 Data Filtering	16
5. Results	20
5.1 Climatology	20
5.2 Dual Doppler vs reference	21
5.3 Sector scan vs reference	23
6. Discussion – one lidar or two?	27
7. Conclusion	27
References	29
Acknowledgements	30

Summary

Long range scanning lidars have the ability to be deployed along the coastline to measure the near shore wind resource. Within the wind energy scope, this is most applicable to assessing the potential energy production (and thus revenue) of a prospected near shore wind farm (here defined as 3-12km from the coast). Ground based remote sensing has numerous advantages over traditional in-situ (offshore met mast) and buoy based installations, mainly in terms of cost, complexity, and failure/delay risk. Since each lidar can only measure a portion of the wind vector, it is necessary to either deploy two devices in tandem (dual Doppler) or employ a single Doppler scanning strategy such as PPI (plan position indicator, or sector scan) which allows for estimation of the two component horizontal wind vector. In preparation for a six month long measurement campaign along the Danish North Sea, a one week experiment was performed at DTU's test centre for large wind turbines (Høvsøre), which lies 1.8km inland and consists of flat terrain with predominate winds from offshore. Two lidars in staring dual Doppler mode and one lidar performing 60 degree sector scans had their beams collocated atop a 116.5m met-mast, which provided reference wind speed and direction values. The 10 minute reconstructed lidar measurements were in excellent agreement with the reference instrumentation. The dual Doppler results matched within 0.1% of the reference wind speed, with very low levels of unbiased scatter. Sector scan results also indicate very good agreement with the met-mast, corresponding within 0.2% for wind speed, with an R^2 of 0.998. The sector scan results for wind speed exhibit larger amounts of scatter than with dual Doppler, however the bias is centred around the regression line which gives good indication that wind measurements taken using the sector scan method are valid and acceptable for use in performing wind resource studies in simple terrain and in offshore conditions. Further, we show that when measuring in these cases, a sector size of 38 degrees still measures within 0.6% of the reference data for wind speed.

1. Introduction

1.1 The need for near-coastal wind data

The political and social unpopularity of land-based wind turbines witnessed in most of northern Europe, is driving a search for more and more offshore wind farm locations. Since many of the ideal sites (with shallow water, good wind resource and lack of dominating, conflicting interests) have already been developed, the search moves to the second rank which can include both closer to shore (poorer resources but lower development costs) or further offshore (better resource but higher costs) locations. It is this first group we are primarily interested in with this report – the so-called ‘near coastal’ wind farms that loosely defined, are between 3 and 12 km off the coast.

A second trend relevant to this report, which we are currently witnessing, is the technical and commercial acceptance of scanning lidars. By ‘scanning lidars’ we mean wind speed measuring lidars that have a scanning head allowing the trajectory to be (within the system’s kinematic constraints) arbitrarily chosen as opposed to being completely defined by the construction (see (Vasiljević, 2014) and Figure 1). We are concerned in the RUNE project and this report with using coastally placed (ground based) scanning lidars to measure the near coastal (offshore) wind resource (Courtney and Simon, 2016). Examples of relevant scanning lidars include the Lockheed Martin Windtracer, the Leosphere Windcube W400S and a long range scanning lidar from Mitsubishi Electric.



Figure 1: WindCube 200S dual-axis scanner head

Source: (Simon, 2015)

The common link between the emergence of scanning lidars and the increasing interest in near-coastal wind farms is the possibility of placing such lidars at relevant coastal sites with the task of providing wind resource data in the potential near-coastal wind farm areas. Such data would be used to improve the accuracy of resource estimates from mesoscale modelling (e.g. WRF) without having to incur the high cost of deploying fixed offshore measuring masts. The feasibility of this concept is being studied in the RUNE project.

1.2 Goal of this report

All wind lidars share the limitation that they are only able to measure the wind speed projected along the line in which they are pointing their laser beam (the so-called ‘radial speed’). In order to obtain the horizontal wind speed and direction, it is necessary either to measure in more than one direction and assume that the lidar is measuring different projections of the same wind speed or to measure with more than one laser beam originating from different positions. In both cases the radial speeds obtained from the different projection angles can be used to derive the wind speed vector.

Long range scanning lidars can thus be used in a number of different ways for measuring the offshore wind. One scanning lidar can be used in plan position indicator (PPI), or ‘sector scanning’ mode, (Figure 2, left pane) in which the lidar scans along an arc of typically 30-60° and derives the wind speed and direction from the variation of the radial speed. Alternatively, two spatially separated lidars can be used to measure the wind speed at the intersection of their beams (Figure 2, right pane). This is known as ‘dual Doppler’ mode.

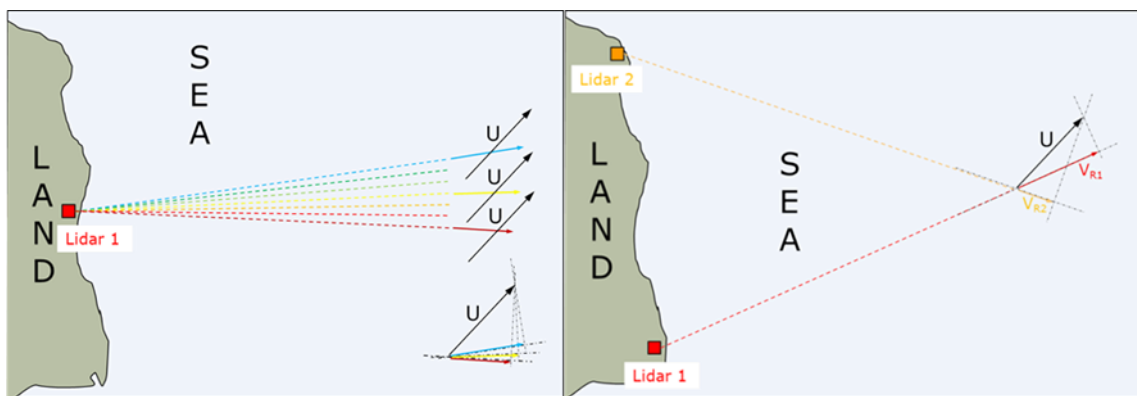


Figure 2 Coastal scanning lidar. Left- sector scanning, Right- dual Doppler configuration

Scanning lidars are expensive (approximately 0.5MM €) so the price of even a short (3 month) campaign with one lidar could well exceed 100k € alone in rental costs. The same measurement campaign with two lidars will be close to twice as expensive (there will be small savings in travelling expenses). If one lidar performing sector-scans is sufficient to measure the wind resource, the money saved could essentially lower development costs, or provide measurements at a second location.

The purpose of this report is to investigate whether one or two lidars are necessary for a coastal wind campaign. This will be achieved by comparing the results from simultaneous sector-scanning and dual-Doppler measurements on shore at a near-coastal site where wind speed measurements from a high quality reference mast are available.

1.3 Structure of this report

In the following section, the basic concepts of sector-scanning and dual Doppler measurements will be presented together with a mathematical outline of their reconstruction methods. Section 3 describes the Sector Scanning vs. Dual Doppler (SSvsDD) measurement campaign, including a site description, details of the lidars and their configurations as well as a description of the reference instrumentation. In section 5, comparisons of wind speeds and directions measured with the two lidar systems are made to

the reference wind speed and direction measurements. These results are used as the basis for the discussion of the relative merits of deploying one or two lidars in section 6. Conclusions from the experiment are given in sections 6 and 7.

2. Measuring wind speeds using scanning lidars

2.1 General remarks

The most generalised form of wind speed retrieval of a 3D wind speed vector (u, v, w) is to have 3 radial wind speeds at the point of interest. In this manner, the wind speed vector can be determined explicitly, without the need for any assumptions about the homogeneity of the flow. Measuring in this configuration is referred to as triple Doppler and requires three spatially separated devices with their beams synchronised in both space and time. When performing a commercial wind resource assessment, we are most interested in characteristics of the horizontal flow field (components u and v).

The magnitude of the wind components (u_r) projected along the line of sight to the lidar in the zero degree elevation case is given by:

$$u_r (m/s) = u_h * \cos \theta$$

Where u_h represents the true wind speed and θ represents the angle between the wind direction and the line of sight of the lidar's optical system.

Therefore, when the wind direction is aligned with the line of sight such that $(\theta = 0 \text{ or } 180^\circ)$, the radial velocity will represent the true (or negated) wind speed. For cases where the wind direction is perpendicular $(\theta = 90 \text{ or } 270^\circ)$ such that $\cos \theta = 0$, there will be no component projected along the LOS, and the lidar will be unable to measure any portion of the wind.

Once solutions are obtained for u and v , they can be transformed to the familiar scalar horizontal wind speed value:

$$u_h (m/s) = \sqrt{u^2 + v^2}$$

Lastly, the wind direction is obtained using the two argument inverse tangent function (atan2). This is due to necessary inputs on the component signs (+/-) and limitations with the single argument (arctangent) function returning undefined values when $u = 0$. It is important to note that the result is expressed in mathematical terms and not according to meteorological notation.

$$dir (degrees) = \text{atan2}(u, v) * \frac{180}{\pi}$$

2.2 Dual Doppler

2.2.1 Fundamentals

Often, such as the case offshore and when utilising low elevation angles, the vertical wind component w is close to zero and can be reasonably ignored. In this case, we need only two radial wind speeds in order to explicitly solve for the 2D wind vector (u, v) . This is the case shown in Figure 2, right pane. Intuitively we can see that the angle between the two beams needs to be sufficiently large that the difference in magnitude of the measured radial speeds is also large (but not so large as to introduce error when the wind direction is perpendicular to the laser path). In practice, this means that the spacing between the lidars needs to be of the same order as the distance to the point of interest from each of the lidars (in order to achieve an optimal 90 degree opening angle at the focus point).

For a near-coastal wind speed measurement at 10km offshore, the two lidars would need to be placed at least 6km apart. This requires an additional site selection, additional power logistics and the necessary software and communication infrastructure to allow synchronised measurements to be made from the two lidars.

2.2.2 Reconstruction method for speed and direction

The dual Doppler retrieval algorithm used in our analysis is as follows:

For each lidar index i (#1 or 2), the radial speed measurement u_{ri} can be used to obtain estimations of the vector components (u, v, w) of the 3D wind speed.

$$u_{ri} = u \sin \theta_i \cos \varphi_i + v \cos \theta_i \cos \varphi_i + w \sin \varphi_i$$

Where θ represents the azimuth angle and ϕ represents the elevation angle of each respective lidar.

Since the elevation angles used in the experiment are sufficiently small, we can assume that the vertical component w does not contribute to the observed radial speed vector and discard it. The formulas for obtaining u and v estimates are given from (Newsom, 2015), where \hat{u}_{ri} represents the radial velocity obtained through the lidar measurement process:

$$u = \frac{\hat{u}_{r1} \cos \theta_2 \cos \varphi_2 - \hat{u}_{r2} \cos \theta_1 \cos \varphi_1}{\cos \varphi_1 \cos \varphi_2 (\sin \theta_1 \cos \theta_2 - \sin \theta_2 \cos \theta_1)}$$

$$v = \frac{\hat{u}_{r2} \sin \theta_1 \cos \varphi_1 - \hat{u}_{r1} \sin \theta_2 \cos \varphi_2}{\cos \varphi_1 \cos \varphi_2 (\sin \theta_1 \cos \theta_2 - \sin \theta_2 \cos \theta_1)}$$

Once solutions for u and v are obtained, they can be combined using the approach outlined in section 2.1 to obtain the horizontal wind speed and direction.

2.3 Sector scanning (partial PPI)

2.3.1 Fundamentals

If there are good reasons to assume that the horizontal wind speed and direction will be essentially homogeneous over a certain area, we can assume that one lidar scanning over the area in an arc will measure different projections of the same horizontal wind speed. This is the concept illustrated in Figure 2, left pane. Reconstructing the wind vector components (as demonstrated in the next section) reduces

to a problem of fitting the measured radial wind speeds to a sine function in which the amplitude will give wind speed and the phase provides the wind direction.

2.3.2 Sector scan reconstruction methods

There are numerous methods to reconstruct horizontal wind speed and direction from LOS measurements in a single Doppler PPI scenario. The core idea is that for a single lidar to obtain estimations for u and v , multiple spatially separated points must be sampled. This is because at minimum, two radial speed measurements are necessary to obtain estimates of u and v .

Two main approaches exist for sector scan reconstruction: Variational Assimilation (mathematical minimisation of an error/cost function to produce lowest expected variances), and simple statistical/geometric fitting, such as VAD or Velocity Azimuth Processing (VAP). We will employ the simplified models in this analysis.

The simplest approach for sector scans (PPI of less than 360 degrees) is to use the integrated, or extended VAD reconstruction algorithm. Radial speed data is point processed to fit to a sinusoidal curve. The fitted function has the representative properties: amplitude = wind speed, phase = wind direction, and offset = vertical velocity (Browning, 1968).

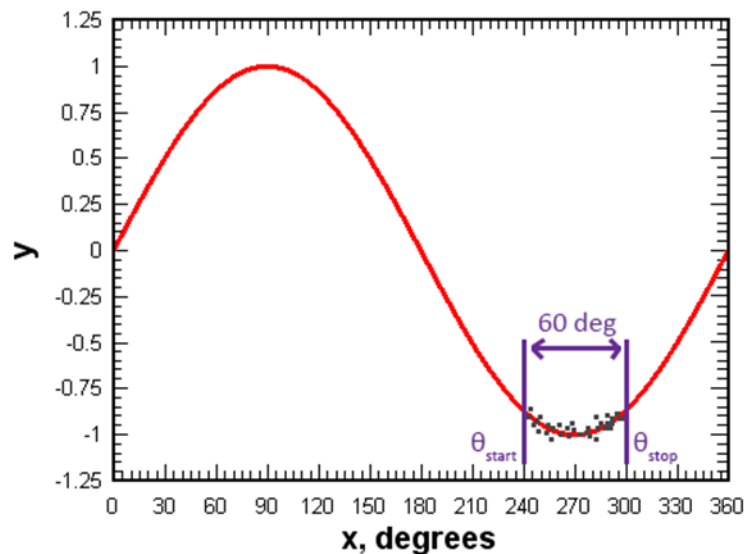


Figure 3: Point process fitting of radial speed values to sine function from 60° sector scan

The highest or lowest point of the sine wave represents the best fitting area to estimate amplitude (wind speed), as it provides the minimum/maximum point and most distinctive shape along the curve. Therefore the reconstruction algorithm results in the lowest measurement error at the peak and trough of the fitted trigonometric function.

As a reminder from what was mentioned in section 2.3.1, the horizontal wind conditions (e.g. speed, direction and composition) over the scanned area must be considered uniform in order to solve the equations.

The simplest VAP approach only takes into account the start and end measurement points of the scanned arc. The points are fit to a sine curve using a trigonometric least squares regression, in which the residuals of the fitted points are minimised.

$$\bar{u} = \frac{\hat{u}_{r1} \sin(\theta_1) - \hat{u}_{r2} \sin(\theta_2)}{\sin(\theta_1 - \theta_2)}$$

$$\bar{v} = \frac{\hat{u}_{r1} \cos(\theta_1) - \hat{u}_{r2} \cos(\theta_2)}{\sin(\theta_1 - \theta_2)}$$

An improvement on this simplified model is extending the formula to include measurements over the entire scanned area (i.e. integrating the elements from the start to stop azimuth range). In practice, this results in a summation of the angularly separated LOS velocities. The formulas for obtaining u and v estimates using the integrated VAP method are given below:

$$\bar{u} = \frac{(\sum_{\theta_{start}}^{\theta_{stop}} (\hat{u}_r * \cos \theta) * \sum_{\theta_{start}}^{\theta_{stop}} (\sin^2 \theta)) - (\sum_{\theta_{start}}^{\theta_{stop}} (\hat{u}_r * \sin \theta) * \sum_{\theta_{start}}^{\theta_{stop}} (\cos \theta * \sin \theta))}{((\sum_{\theta_{start}}^{\theta_{stop}} \cos^2 \theta) * \sum_{\theta_{start}}^{\theta_{stop}} \sin^2 \theta) - (\sum_{\theta_{start}}^{\theta_{stop}} (\cos \theta * \sin \theta))^2)}$$

$$\bar{v} = \frac{(\sum_{\theta_{start}}^{\theta_{stop}} (\hat{u}_r * \sin \theta) * \sum_{\theta_{start}}^{\theta_{stop}} (\cos^2 \theta)) - (\sum_{\theta_{start}}^{\theta_{stop}} (\hat{u}_r * \cos \theta) * \sum_{\theta_{start}}^{\theta_{stop}} (\cos \theta * \sin \theta))}{((\sum_{\theta_{start}}^{\theta_{stop}} \cos^2 \theta) * \sum_{\theta_{start}}^{\theta_{stop}} \sin^2 \theta) - (\sum_{\theta_{start}}^{\theta_{stop}} (\cos \theta * \sin \theta))^2)}$$

Once estimates for u and v are calculated, we can obtain the horizontal wind speed and direction using the equations presented in section 2.1.

3. The measurement campaign

3.1 Site description

Measurement data used in this experiment was collected at the Danish National Test Centre for Large Wind Turbines at Høvsøre, on the Western coast of the Jutland peninsula in Western Denmark. The site is administered by DTU Wind Energy, with offices located at: Bøvlingvej 41B 7650 Bøvlingbjerg, DK (UTM: 32V, 447901.40 m E, 6256574.19 m N).

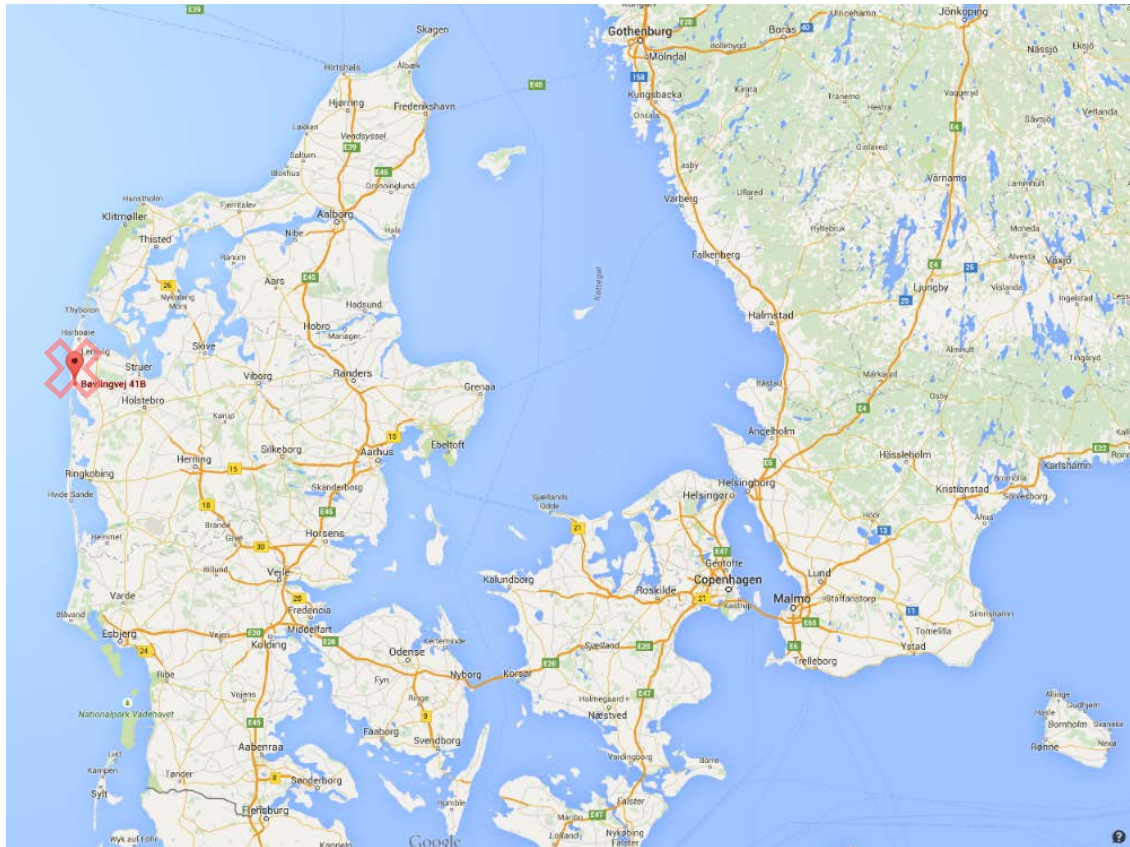


Figure 4: Location overview of Høvsøre Test Station

The site was chosen for its extensive instrumentation, technician support, and history of validated and published literature which will be referred to in the review section. This helps to minimise the amount of unforeseen parameters which can affect the results of the study.

The Høvsøre site consists of flat, simple terrain with only small elevation changes nearby. The maximum elevation is 3m (max slope 2.6%) and minimum -1m (min slope -2.5%). Met mast #6 lies at 0m elevation and 0% slope.

Directly west of the site (1.45 – 2km) lies the North Sea. At the coastline, there is a small dune running parallel to the shore with maximum elevation of 3m (min 0m) and maximum slope of 3% (min -3.8%). The maximum height occurs directly west of met-mast #3 (at 260 degrees to met-mast #6).

From the terrain conditions, wind climatology, and inflow directions considered, the test site at Høvsøre can be considered to have similar conditions to that of the coastal zone where we wish to measure the near shore wind resource.



Figure 5 Overview of the site location and terrain composition, showing the North Sea, Bøvling Fjord and city of Bøvlingbjerg. The brightened thatched region (118-270°) represents wake free inflow.

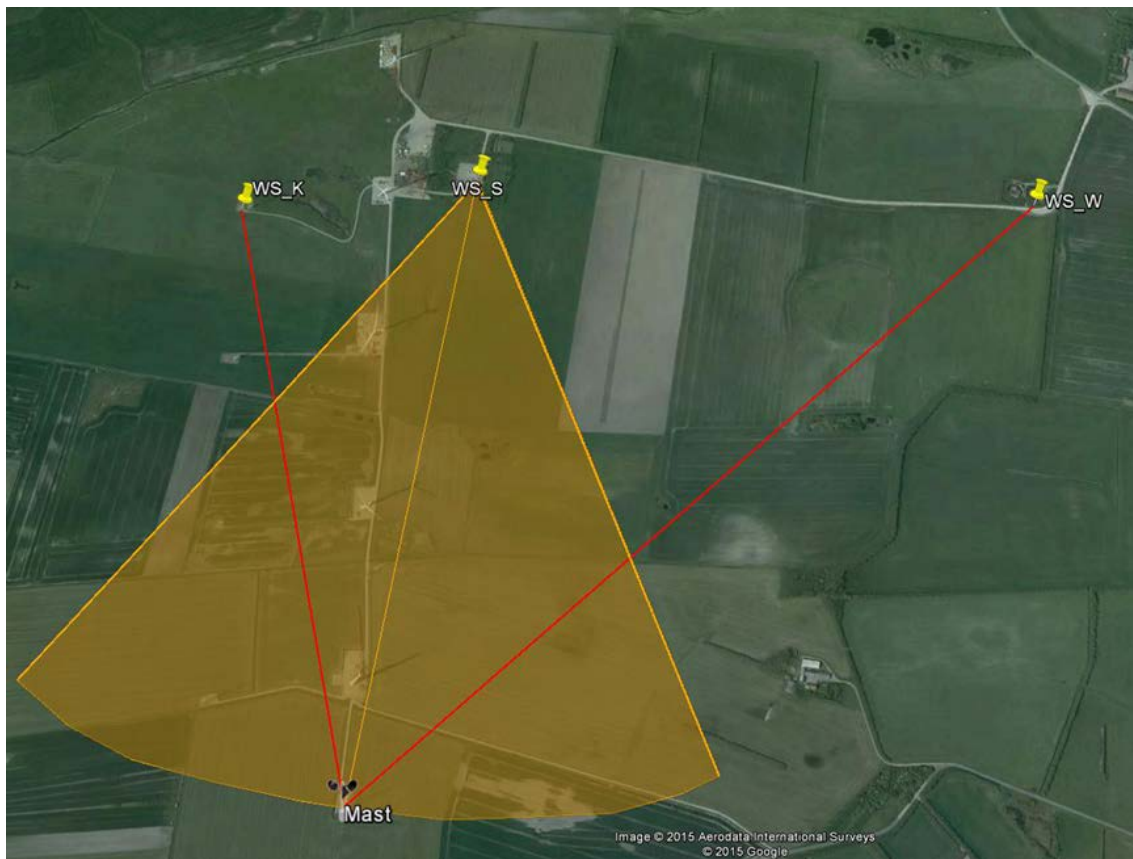


Figure 6 Scanning strategies performed during the SSvsDD experiment

3.2 The instrumentation

The Høvsøre test site consists of 5 turbine stands, each with a respective met-mast located directly west. There is also a tall met-mast (116.5m) located at the south end of the site near the lidar calibration pad. Additionally, there are two 160m aircraft warning light towers to the east of the north & south turbine stands. Each structure is shown below in the site layout overview.

The cup anemometer mounted at the top of mast 6 (116.5m) was used as the reference wind speed measurement. This is a WindSensor P2546-OPR cup anemometer calibrated in the German Windguard wind tunnel (certificate included in Appendix). In addition to the calibration uncertainty, components relating to the uncertainty introduced by the mounting of the cup on the mast (0.25% mounting uncertainty) and by the classification of the cup anemometer must be added. A typical standard uncertainty at 10 m/s corresponds to about 0.1 m/s in wind speed measurement.

The reference wind direction is taken from a boom mounted wind vane at 100m on the south side of the same tower. This wind direction has been cross checked against a sonic anemometer also at 100m, but boom-mounted on the north side of the mast. A simple linear regression between the two showed very good agreement, with no offset or bias overall.

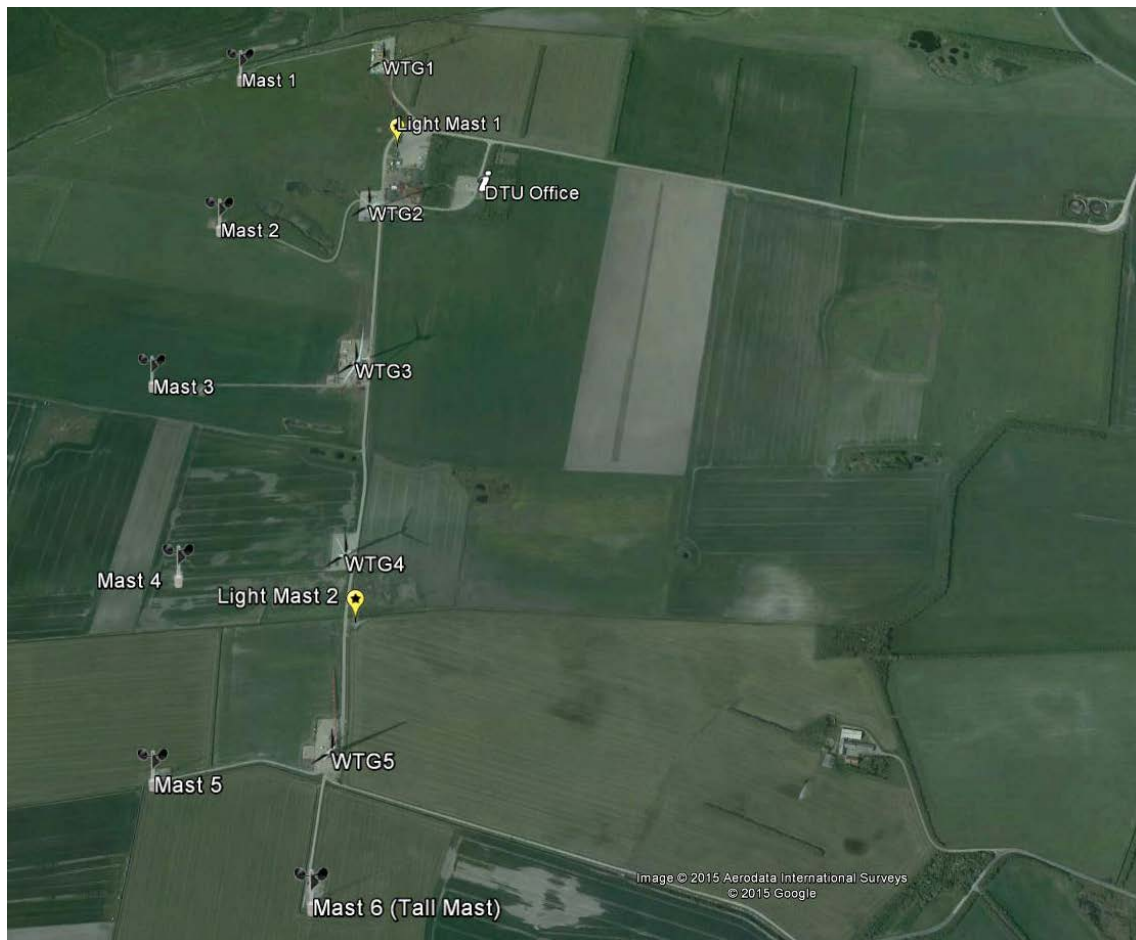


Figure 7 Overview of the Høvsøre test site layout

Three WindScanners were deployed within the campaign. Two devices (WS_K: Košava and WS_W: Whittle) were set-up in dual Doppler mode, with a 63 degree opening angle intersecting 10cm above the southernmost met-mast. The other (WS_S: Sterenn) was configured in 60 degree sector scan mode, with the centre of the measuring arc passing directly over the reference cup anemometer. Wind direction measurements were taken from a wind vane mounted at 100m on the same tower, verified using a sonic anemometer also placed at 100m.

Geospatial coordinates for the devices were measured using differential GPS with an accuracy of 10cm. The results are presented in the following table (UTM system, Zone 32V):

Table 1: SSvsDD deployment positions

Object	Easting (m)	Northing (m)	Height (m)	Elevation Angle (degrees)
WS_K	447450.548	6256541.135	4.054	6.1
WS_S	447893.983	6256558.133	5.078	5.96
WS_W	448937.717	6256404.894	5.409	4.25
116.5m Met-Mast (base)	447647.39	6255435.76	4.836	N/A

Further, technical parameters of the scanning strategies for each lidar are given in the following tables:

Table 2: Lidar configuration (Sterenn)

WindScanner Sterenn : Property	Value
Scan type:	PPI (sector scan)
Sector size:	60 degrees
Elevation angle (ϕ):	5.36 degrees
Elevation offset:	0.6 degrees
Azimuth range (θ_{Start} : θ_{Stop}):	150.xxx : 208.xxx (auto-reversing)
Azimuth offset:	12.31 degrees
Linear distance:	1149.14 m
Range gate to cup:	1166 m (41 range gates in total)
Position (UTM):	{447893.983m E, 6256558.133 m N, 5.078 m Height}
Scanning speed:	2.5 degrees / s
Time per scan:	12 s
Azimuth separation:	2 degrees per LOS (30 LOS)
Pulse length:	200 ns
Accumulation time:	400 ms
FFT size:	64

Table 3: Lidar configuration (Koshava)

WindScanner Koshava : Property	Value
Scan type:	Fixed LOS (dual Doppler with Whittle)
Elevation angle (ϕ):	5.32 degrees
Elevation offset:	0.78 degrees
Azimuth angle (θ):	165.66 degrees

Azimuth offset:	3.46 degrees
Linear distance:	1122.76 m
Range gate to cup:	1135 m (41 range gates in total)
Position (UTM):	{447450.548, 6256541.135, 4.054}
Pulse length:	200 ns
Accumulation time:	500 ms
FFT size:	64

Table 4: Lidar configuration (Whittle)

WindScanner Whittle : Property	Value
Scan type:	Fixed LOS (dual Doppler with Koshava)
Elevation angle (ϕ):	3.1 degrees
Elevation offset:	1.15 degrees
Azimuth angle (θ):	229.57 degrees
Azimuth offset:	2.82 degrees
Linear distance:	1613.74 m
Range gate to cup:	1625 m (41 range gates in total)
Position (UTM):	{448937.717, 6256404.894, 5.409}
Pulse length:	200 ns
Accumulation time:	500 ms
FFT size:	64

Additional information including site deployment procedures and hard target mapping can be found within (Simon, 2015).

4. Methodology

4.1 Data Filtering

It is necessary to perform some filtering on the raw lidar data in order to obtain high quality output with which to perform the analysis. Filtering takes places in the following stages:

∞ CNR filter

High CNR values can represent the laser pulse interacting with a hard target, such as a turbine tower, mast structure/guy wires, etc. The difficulty in strict cut-off based CNR filtering is that factors such as aerosol concentration are changing over time and can influence the range of valid CNR values. It is usually apparent from visually comparing the time series graphs of CNR and radial speed over the scan which values are contaminated. A suggested range of -25 to -5dB is usually appropriate, however in this analysis the filtering levels were decided visually (by the operator) within the analysis software. For the SSvsDD campaign, filtering based on both CNR and radial speed usually removes 0.3-2% of the values.

The entire raw and filtered graphs for each set of scans can be found within the appendix of (Simon, 2015). An example of pre and post-processed CNR values are presented in the following figure:

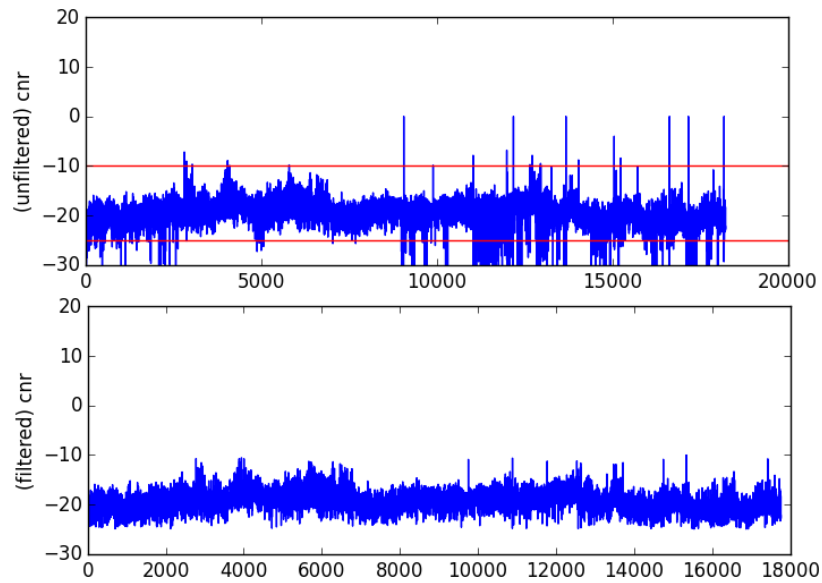


Figure 8 CNR filtering, before and after

∞ Radial speed filter

Often, filtering by CNR alone is not sufficient to remove all spurious LOS measurements from the dataset. This is because CNR filters which are too strict often remove excessive amounts of valid data points, while filters which are too lenient often leave erroneous values. Therefore, a combination of both CNR and radial speed filters was determined to be the best approach.

Since radial speeds in a PPI configuration follow an oscillating (sine wave) pattern, it is also generally simple to find the cut off values by a visual inspection of the radial speed time series graph. Since the magnitude and sign vary depending on wind speed and LOS direction (towards or away from the lidar), it was decided to also determine cut-off limits by hand.

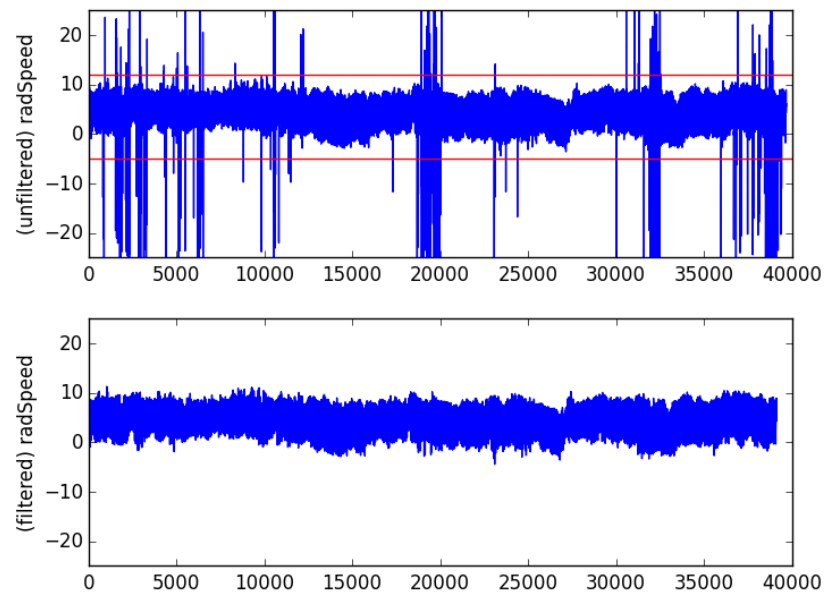


Figure 9 Radial velocity filtering, before and after

∞ Waked wind direction and tower shadow effect filter

Due to the close proximity between the point of measurement (met-mast) and both wind turbines and other light/met masts at the Høvsøre site, it is necessary to perform some additional filtering to remove any possible wake (velocity deficit) or tower shadow effects from influencing the results of the study.

Using the simple Jensen linear wake model, it is possible to determine the range of wind directions from the turbines which need to be filtered. Although the Jensen model's accuracy in near-wake zones is a matter of debate, it provides a good first estimate of the wake expansion scale which can be verified once the linear regression models are run.

$$D_W = D + 2kX$$

Where D_W = the diameter of the downstream turbine wake, D = the diameter of the turbine's rotor plane, k = the wake decay parameter and X = the downstream distance.

Using a k value of 0.075 for flat terrain, we calculate the downstream wake diameter from the furthest turbine on stand #2:

$$D_W = (110m) + (2 * 0.075 * 1131m) \approx 280m$$

And the nearest turbine on stand #5:

$$D_W = (113m) + (2 * 0.075 * 185m) \approx 140m$$

Measuring out the respective wake diameters and removing sectors which could interfere with the measurement volume gives a wake free zone from 118-270 degrees. The tower shadow effect is determined to be fully encapsulated within the turbine wake volume. This result is further verified at the end of the study by plotting the absolute value of the difference between the lidar and reference wind speed against the direction given by the reference wind vane.

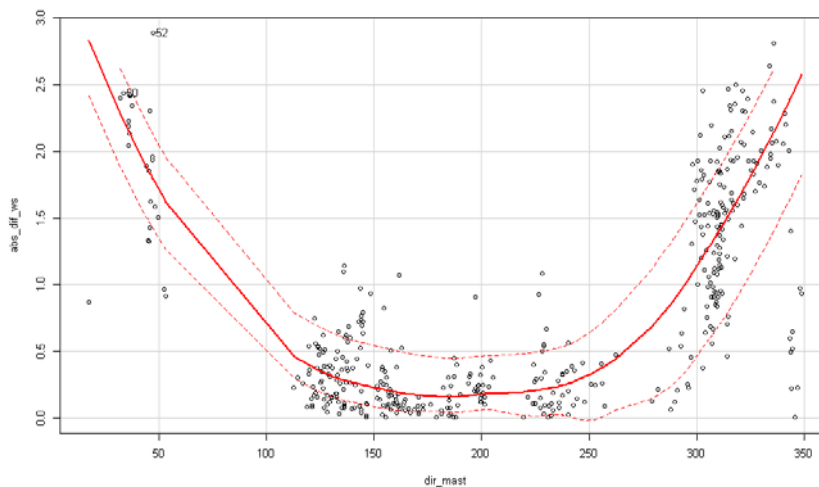


Figure 10 Verification of turbine wake effect from sectors outside 118-270 degrees

∞ Any partial scans (not all LOS) filter – only for sector scan

This filter only applies to the data obtained by sector scanning. After the previous filter functions (CNR and radial speed) have been run on every scenario, the reconstruction function (called ‘fitting’) breaks down (slices) the data-frame into n-sized smaller data-frames, with n being the number of LOS within the scan. In the SSvsDD dataset, this represents a length of 30 rows (60 degree sector size during measurement, with an azimuth separation of 2 degrees per LOS).

The fitting function then inspects the sliced data-frame containing one scan. If any of the LOS values have been filtered out, then the scan is discarded. Otherwise, the program continues on to the next step. Removing partially filtered scans is necessary in order to obtain the highest quality data and be able to examine the effect of reconstruction using smaller sector sizes. In other cases such as normal measurement operation, this step may not be necessary. Typically, 2-20% of scans within each scenario are filtered out in the SSvsDD dataset.

∞ Reduction in sector size filter – only for sector scan

Now that we have only full sector scans remaining with all available LOS radial speeds, the next step is to determine whether the program is being asked to reconstruct using a smaller sector size than the original measurement data (only for the purposes of this study). If so, then the scan is sliced once again into a smaller size of n-rows, where n is the number of LOS desired for the given opening angle. For the case of a 30 degree sector reduction from SSvsDD, the new size will be 16 rows. This is due to a 2 degree separation between each LOS and the way the azimuth values are recorded in the data.

The middle LOS of the unfiltered scan is chosen, and half the new data-frame length is taken in both directions (so as to reduce the sector width symmetrically). In certain cases where the new length is an even number (so it is not possible to reduce the width symmetrically), then 1 additional LOS is included either on the left or right hand side at random.

∞ Availability of scans within 10min average filter

When averaging data over a finite period, a low number of samples can result in a non-uniform distribution of the samples, causing incorrect biasing of the result. Therefore, a parameter is needed in order to determine how trustworthy the time averaged result is. During the resampling process of the analysis software written for this study, a column “avail” is calculated which contains the count of non-null values used to create the binned average. For the purposes of this dataset, we require that at minimum 19 samples (out of a maximum of 50) be available in order to trust the 10 minute averaged output. This is due to larger errors observed with less than 19 samples (38%) used in the averaging calculation.

∞ Wind speed between 4 and 25 m/s filter

For the purposes of the RUNE project, we are only interested in values which are within the operating range of a wind turbine. Therefore, we have chosen wind speed limits which

closely resemble the cut-in and cut-out range of a modern utility scale wind turbine, such as the Siemens model SWT-2.3-93 (Siemens Wind Power, 2015).

5. Results

5.1 Climatology

Using data captured by the numerous instruments mounted on the met-mast, a brief description of the site's wind speed statistics are presented here. For a more detailed report, please refer to (Simon, 2015). Summary statistics from the cup anemometer are shown in the following table:

Table 5: Summary statistics: Wind speed (cup anemometer) at 116.5m over the measurement period

Wind Speed (cup) at 116.5m	Value (m/s)
Minimum	1.799
1 st quartile (middle value between minimum and median)	5.351
Median	7.783
Mean	7.840
3 rd quartile (middle value between median and maximum)	10.292
Maximum	14.577

Along with a time series graph over the measurement period for wind speed:

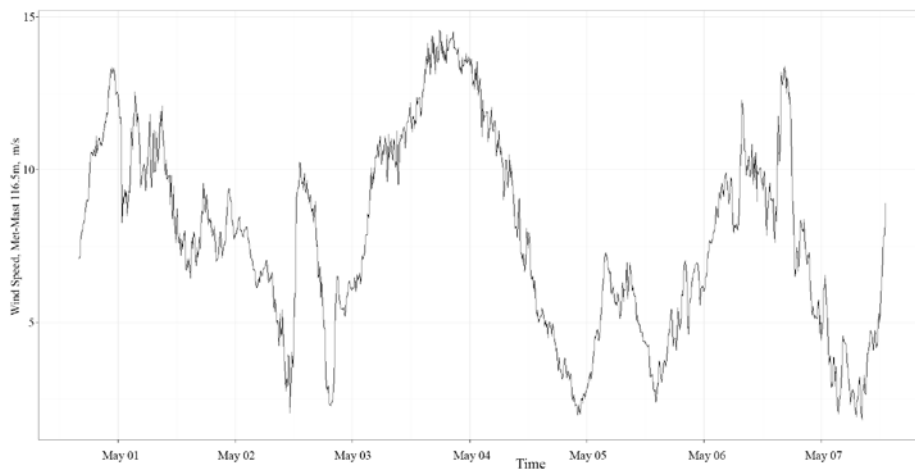


Figure 11 Time series: wind speed, met-mast cup anemometer at 116.5m

And polar wind speed and direction roses over heights 10, 60, 100, and 116.5m:

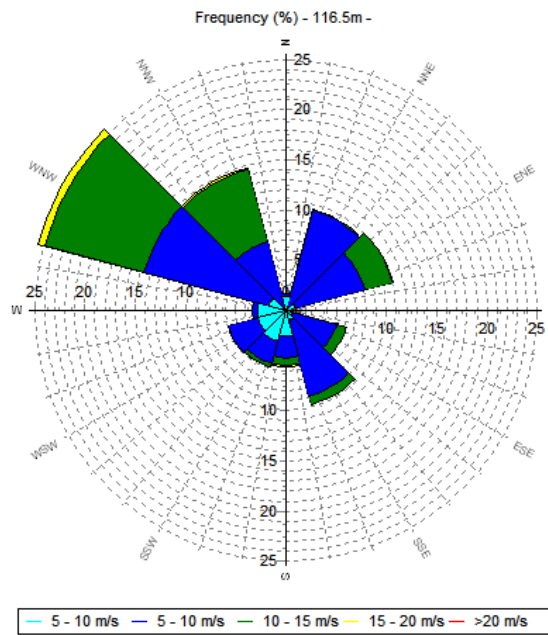


Figure 12 Wind rose at 116.5m, also with corresponding wind speeds for each 10 degree sector

From these results, we show that during the experiment period, the reference instrumentation exhibits no obvious errors, and the data gathered seems plausible to continue with the comparison from lidar measurements.

5.2 Dual Doppler vs reference

The results from the dual Doppler analysis are presented in the following time series graphs for wind speed and direction. 10 minute averaged values are used.

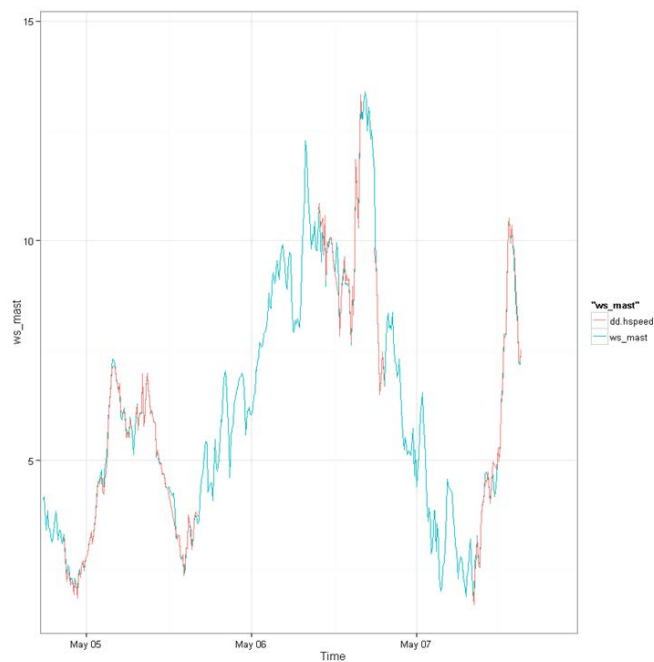


Figure 13 Time series of wind speed: Dual Doppler lidar (red) and mast 116.5m reference (turquoise)

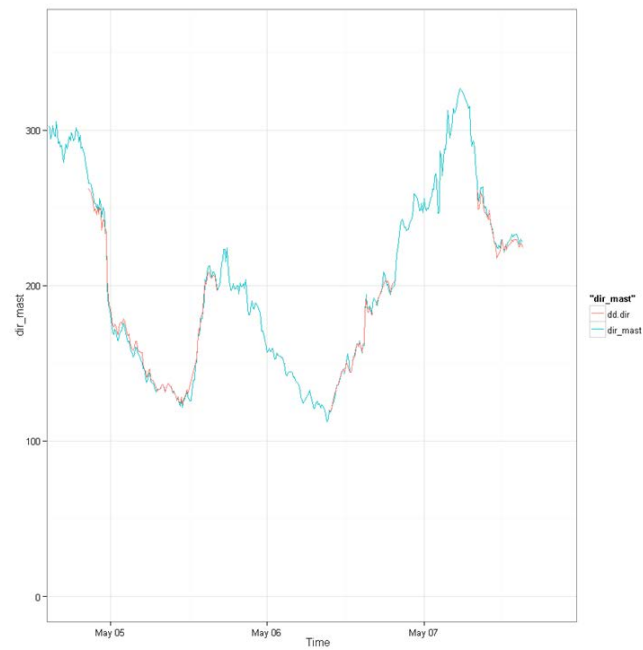


Figure 14 Time series of wind direction: Dual Doppler lidar (red) and 100m mast reference (turquoise)

Scatterplots comparing the 10 minute averaged dual Doppler results to the reference (cup anemometer at 116.5m and wind vane at 100m) are given in the following figures, along with the results of the linear fit models (constrained linear regression for speed and unconstrained linear regression of direction):

$$ws_{LiDAR} = (0.999) ws_{mast} + 0$$

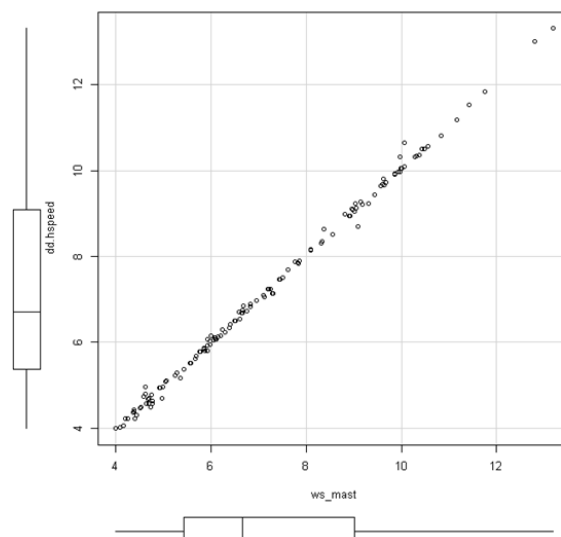


Figure 15 Scatterplot of wind speed: Dual Doppler lidar vs. mast reference (116.5m)

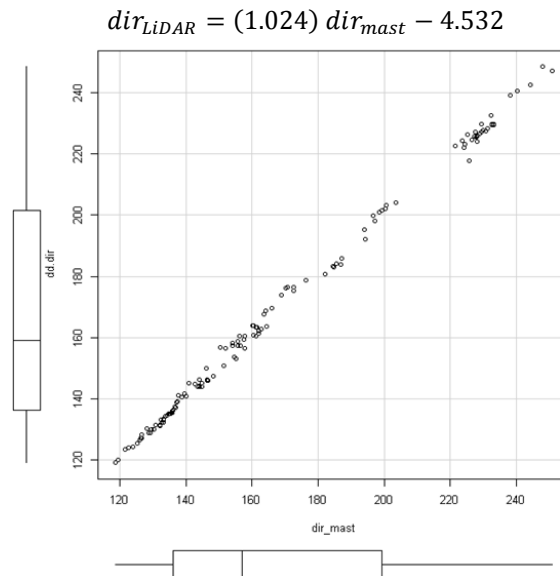


Figure 16 Scatterplot of wind direction: Dual Doppler lidar vs. mast reference (100m)

5.3 Sector scan vs reference

The results from the original (60 degree) sector scan analysis are presented in the following 10 minute averaged time series graphs for wind speed and direction.

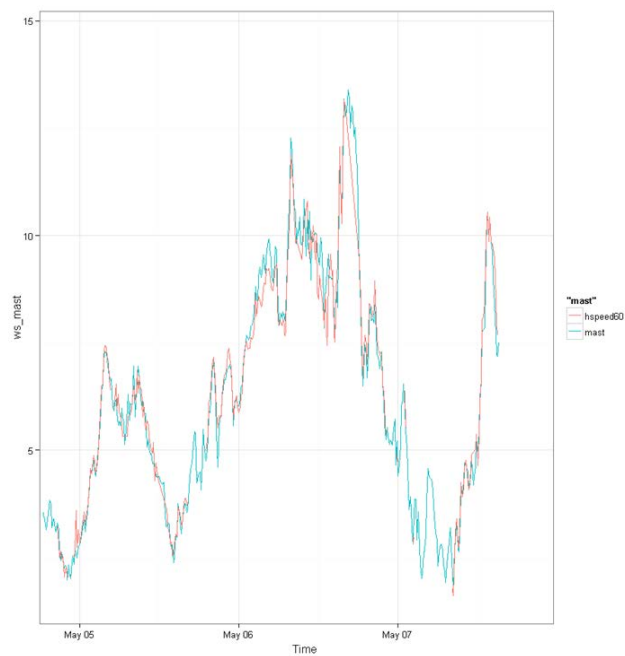


Figure 17 Time series of wind speed: 60 degree sector scan lidar (red) and reference mast cup (turquoise).

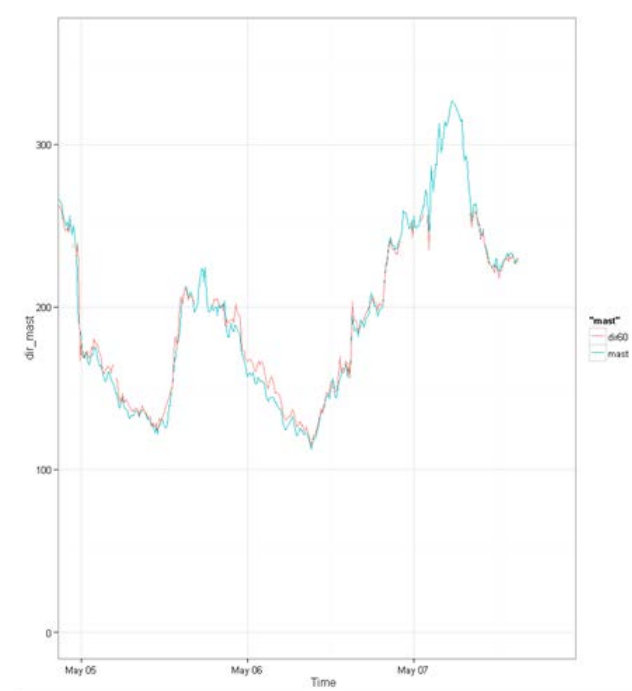


Figure 18 Time series of wind direction: 60 degree sector scan lidar (red) and 100m reference wind vane (turquoise)

Results for the sector scanning lidar are shown for four opening angles: 60, 50, 38, and 30 degrees. The purpose of this is to determine the effect of larger and smaller sector sizes on the: overall shape (linear regression coefficient), overall fit (r^2 coefficient), amount of scatter (residuals) and bias of scatter (under/over prediction).

The plots comparing the reconstructed 10 minute averaged wind speed and direction from the lidar to the collocated cup anemometer and wind vane (reference measurement) are given in the following section. Boxplots are also included along both the x and y axes, which represent (starting from the origin) the minimum, first quartile (middle value between minimum and median), median, third quartile (middle value between median and maximum), and maximum values

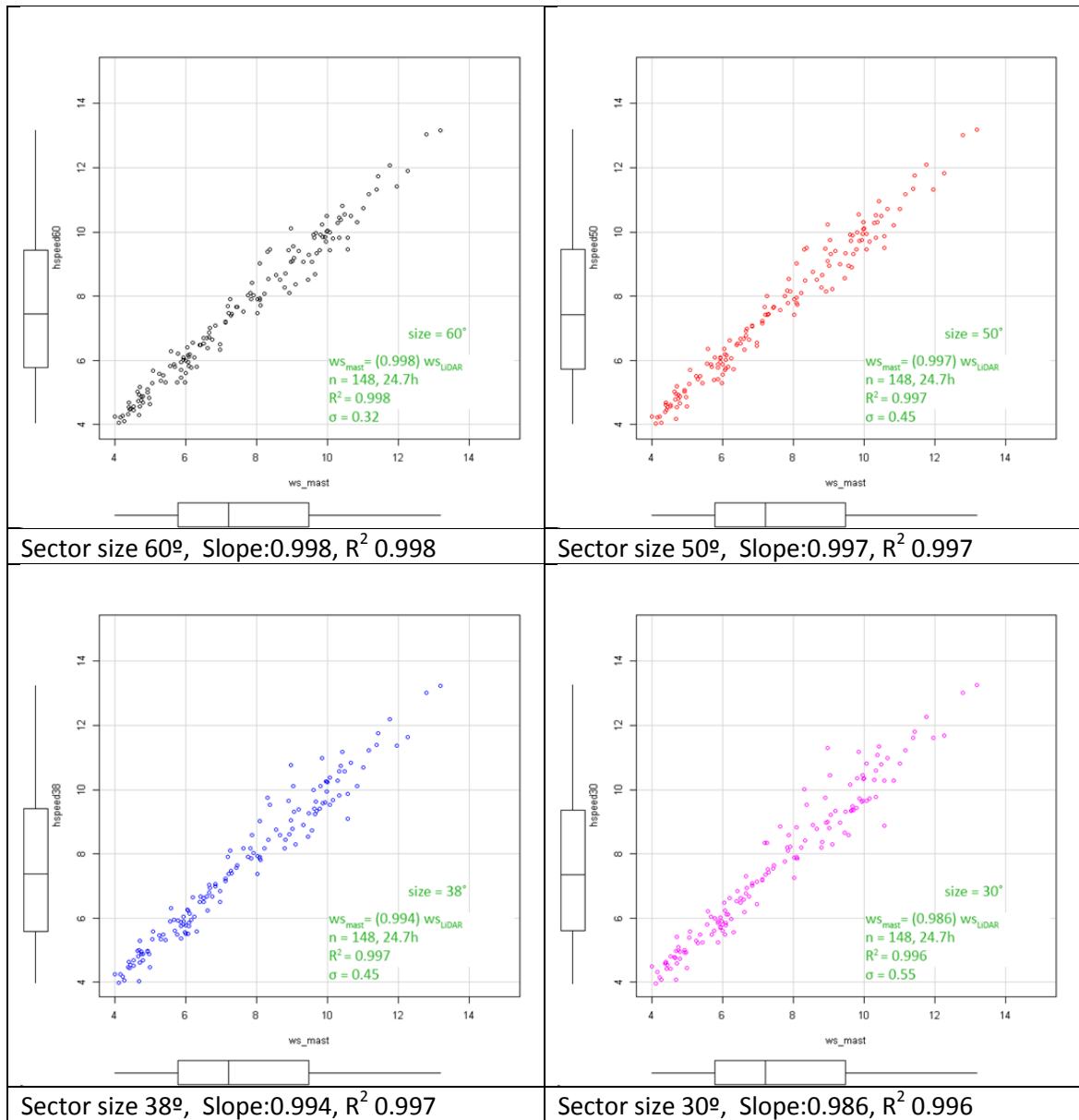


Figure 19 Scatter plots of wind speed: Sector scanning lidar vs reference cup anemometer at 116.5m

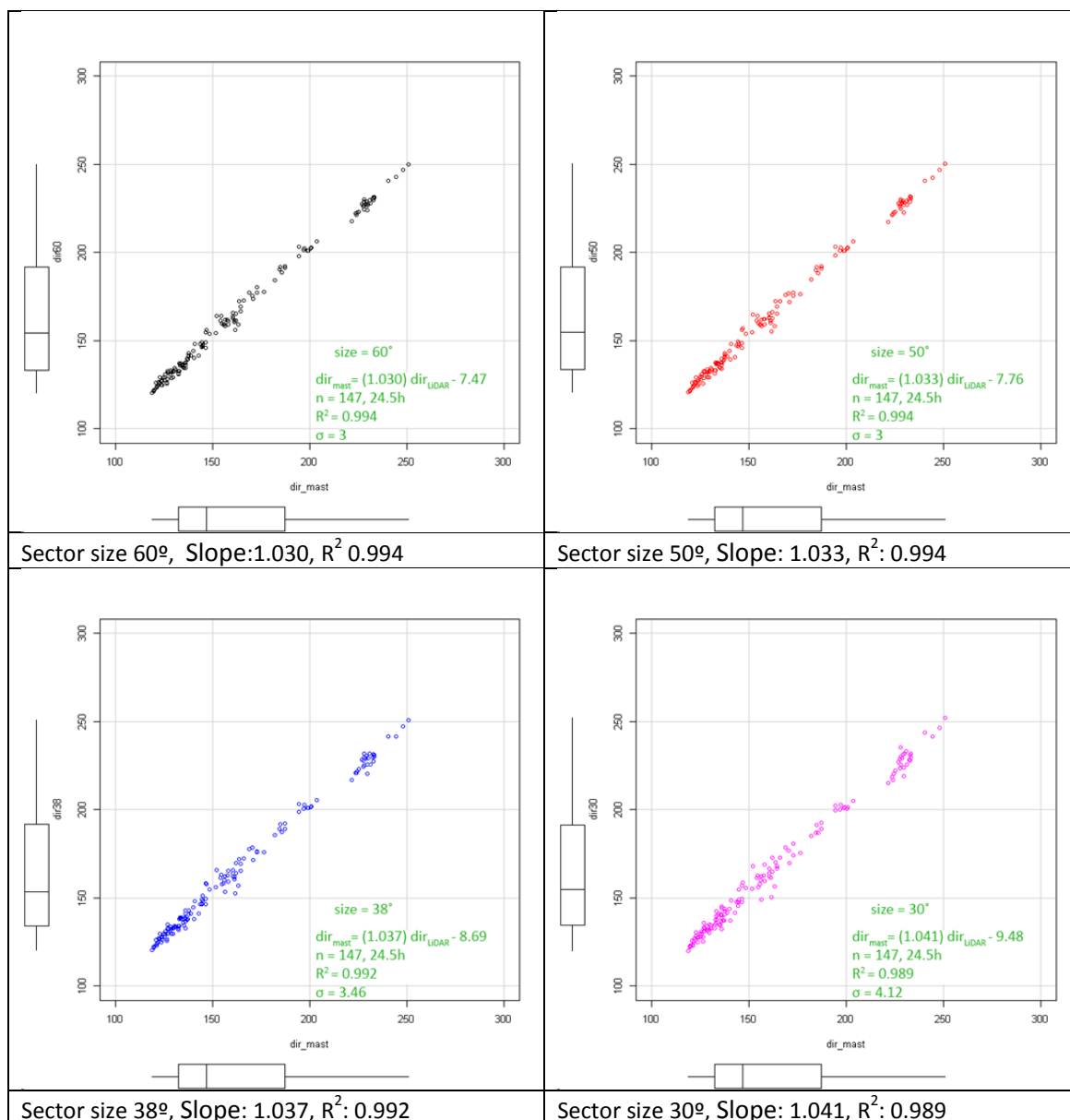


Figure 20 Scatter plots of wind direction: Sector scanning lidar vs reference wind vane at 100m

6. Discussion – one lidar or two?

In section 5, we have seen, as expected, that the dual Doppler (2 lidar) results for the wind speed (Figure 15) show good agreement (within 0.1%) with the reference cup anemometer and very little scatter. Almost as good results are seen for the wind direction (Figure 16). The results for the sector-scanning lidar (Figure 19 and Figure 20) are also very satisfactory with respect to the slope of the fitted regression line. For the largest sector sizes (60 and 50 degrees), the difference between the sector scan and dual Doppler results are only 0.2 and 0.3% respectively. However and again as expected, the scatter was much larger in the sector-scanning case since the correlation between the sector-averaged lidar speed and the point average of the cup anemometer will never be as high as the (close to) point to point comparison of the staring, dual Doppler lidar with the reference anemometer.

For a reliable wind resource estimate, we require an accurate and un-biased mean value. Excessive scatter however, will have significance since it will act to artificially broaden the wind speed distribution, albeit by a small amount. Since the shape of a wind turbine power curve is non-linear, we must also consider the effect of any changes in distribution as it relates to energy production. When the lidar's primary function is to establish the correct level of the mesoscale modelling, it seems unlikely that the broadening effect has any significance.

In terms of terrain homogeneity, the Høvsøre test site can hardly be regarded as representative of true offshore conditions. Due to the proximity of the sea and the lagoon to the south, the land fetch length will vary considerably as a function of wind direction between S and N. Especially for the 60 degree sector size, the lidar is in fact scanning over a length of 1.6km in a coastal transition zone. If we are able to achieve good results with sector-scanning at Høvsøre, the results over the much more homogeneous sea surface should be even better.

7. Conclusion

In conclusion, we have outlined two strategies for remotely measuring wind fields offshore in the near-coastal zone using scanning lidars. A single Doppler technique (requiring only one device) known as sector scanning, and the dual Doppler approach (requiring two devices) have been detailed with their respective best practices as well as equations needed to reconstruct horizontal wind speeds and directions. Further, these two approaches have been compared against each other and calibrated reference instruments in a 7 day field experiment at DTU's test centre for large wind turbines (Høvsøre) next to the Danish North Sea. The results of the comparison show excellent agreement for the dual Doppler measurements in both speed (0.1% error) and direction, with extremely low scatter. The reconstructed sector scan values also match very well on average with the reference devices (0.2% error in wind speed), however with a larger magnitude of scatter than using dual Doppler. Since the scatter is unbiased around the fit line, we can say that the single lidar performing sector scans will produce accurate measurements in both wind speed and direction on 10 minute averaged scales. Further, by filtering out certain lines of sight within the sector scans (thus artificially decreasing the angular width), we have shown that even with smaller sector sizes of 38°, the error in wind speed measurements is only 0.6%. These results apply equally for wind direction. For commercial purposes of prospecting a

potential near-shore development site, it is then considered sufficient to deploy a single lidar with a sector scan trajectory to obtain an accurate measurement of the wind climate.

References

1. Browning, K.A., Wexler, R., 1968. *The Determination of Kinematic Properties of a Wind Field Using Doppler Radar*. J. Appl. Meteor. 7, 105–113. doi:10.1175/1520-0450(1968)007<0105:TDOKPO>2.0.CO;2
2. Courtney, M & Simon, E 2016, *Deploying scanning lidars at coastal sites*. DTU Wind Energy. DTU Wind Energy E, vol. 0110
3. Newsom, R.K., Berg, L.K., Shaw, W.J., Fischer, M.L., 2015. *Turbine-scale wind field measurements using dual-Doppler lidar*. Wind Energy 18, 219–235. doi:10.1002/we.1691
4. Simon, E. (2015). Determination of an Optimum Sector Size for Plan Position Indicator Measurements using a Long Range Coherent Scanning Atmospheric Doppler LiDAR. Uppsala University MSc Thesis. Available at: http://orbit.dtu.dk/files/125274101/Thesis_Elliot_DTU_final.pdf
5. Vasiljević, N. 2014; *A time-space synchronization of coherent Doppler scanning lidars for 3D measurements of wind fields*. DTU Wind Energy PhD 0027(EN). ISBN 978-87-92896-62-9

Acknowledgements

This work has been performed under ForskEL project RUNE (journal number 12263). The authors also wish to acknowledge the technical staff both at DTU-Risø and Høvsøre Test Station for their assistance in deploying and monitoring the instruments used in this experiment. Further, we would like to recognise the vast contributions made by Nikola Vasiljević and Guillaume Lea in the development and testing of the long range WindScanner systems.

DTU Wind Energy is a department of the Technical University of Denmark with a unique integration of research, education, innovation and public/private sector consulting in the field of wind energy. Our activities develop new opportunities and technology for the global and Danish exploitation of wind energy. Research focuses on key technical-scientific fields, which are central for the development, innovation and use of wind energy and provides the basis for advanced education at the education.

We have more than 240 staff members of which approximately 60 are PhD students. Research is conducted within nine research programmes organized into three main topics: Wind energy systems, Wind turbine technology and Basics for wind energy.

Danmarks Tekniske Universitet

DTU Vindenergi

Nils Koppels Allé

Bygning 403

2800 Kgs. Lyngby

Telephone 45 25 25 25

info@vindenergi.dtu.dk

www.vindenergi.dtu.dk

akkreditiert durch die / *accredited by the*

Deutsche Akkreditierungsstelle GmbH

als Kalibrierlaboratorium im / *as calibration laboratory in the*

Deutschen Kalibrierdienst



Kalibrierschein
Calibration certificate

Calibration mark

1106 / 3140



1413414

D-K-
15140-01-00

06/2014

Gegenstand <i>Object</i>	Cup Anemometer
Hersteller <i>Manufacturer</i>	WindSensor DK-4000 Roskilde
Typ <i>Type</i>	P2546A-OPR
Fabrikat/Serien-Nr. <i>Serial number</i>	5543 3140
Auftraggeber <i>Customer</i>	Risoe DTU DK-4000 Roskilde
Auftragsnummer <i>Order No.</i>	VT140675
Anzahl der Seiten des Kalibrierscheines <i>Number of pages of the certificate</i>	3
Datum der Kalibrierung <i>Date of calibration</i>	26.06.2014

Dieser Kalibrierschein dokumentiert die Rückführung auf nationale Normale zur Darstellung der Einheiten in Übereinstimmung mit dem Internationalen Einheitensystem (SI).

Die DAkkS ist Unterzeichner der multilateralen Übereinkommen der European co-operation for Accreditation (EA) und der International Laboratory Accreditation Cooperation (ILAC) zur gegenseitigen Anerkennung der Kalibrierscheine.

Für die Einhaltung einer angemessenen Frist zur Wiederholung der Kalibrierung ist der Benutzer verantwortlich.

This calibration certificate documents the traceability to national standards, which realize the units of measurement according to the International System of Units (SI).

The DAkkS is signatory to the multilateral agreements of the European co-operation for Accreditation (EA) and of the International Laboratory Accreditation Cooperation (ILAC) for the mutual recognition of calibration certificates.

The user is obliged to have the object recalibrated at appropriate intervals.

Dieser Kalibrierschein darf nur vollständig und unverändert weiterverbreitet werden. Auszüge oder Änderungen bedürfen der Genehmigung sowohl der Deutschen Akkreditierungsstelle als auch des ausstellenden Kalibrierlaboratoriums. Kalibrierscheine ohne Unterschrift haben keine Gültigkeit.

This calibration certificate may not be reproduced other than in full except with the permission of both the German Accreditation Body and the issuing laboratory. Calibration certificates without signature are not valid.

Datum
Date

26.06.2014

Leiter des Kalibrierlaboratoriums
Head of the calibration laboratory

Dipl. Phys. D. Westermann

Bearbeiter
Person in charge

Techniker Dirk Henniges

Kalibriergegenstand

Object

Cup Anemometer

Kalibrierverfahren

Calibration procedure

IEC 61400-12-1 – Power performance measurements of electricity
producing wind turbines – 2005-12
ISO 3966 – Measurement of fluid in closed conduits – 2008-07

Ort der Kalibrierung

Place of calibration

Windtunnel of Deutsche WindGuard, Varel

Messbedingungen

Test Conditions

wind tunnel area ¹⁾	10000 cm ²
anemometer frontal area ²⁾	220 cm ²
diameter of mounting pipe ³⁾	27 mm
blockage ratio ⁴⁾	0.022 [-]
blockage correction ⁵⁾	1.000 [-]

Umgebungsbedingungen

Test conditions

air temperature	22.7 °C	± 0.1 K
air pressure	1015.6 hPa	± 0.3 hPa
relative air humidity	46.9 %	± 2.0 %

Akkreditierung

Accreditation

01/2013

Anmerkungen

Remarks

Auswertesoftware

Software version

7.62

¹⁾ Querschnittsfläche der Auslassdüse des Windkanals

²⁾ Vereinfachte Querschnittsfläche (Schattenwurf) des Prüflings inkl. Montagerohr

³⁾ Durchmesser des Montagerohrs

⁴⁾ Verhältnis von 2) zu 1)

⁵⁾ Korrekturfaktor durch die Verdrängung der Strömung durch den Prüfling

Anmerkung: Aufgrund der speziellen Konstruktion der Messstrecke ist keine Korrektur nötig.

Remark: Due to the special construction of the test section no blockage correction is necessary

Dieser Kalibrierschein wurde elektronisch erzeugt

This calibration certificate has been generated electronically

Kalibrierergebnis:

Result:

File:	1413414	
Test Item	Tunnel Speed	Uncertainty (k=2)
Hz	m/s	m/s
6.271	4.085	0.050
9.469	6.038	0.055
12.451	7.882	0.050
15.450	9.720	0.051
18.587	11.663	0.057
21.707	13.624	0.051
24.928	15.576	0.057
23.253	14.550	0.051
20.212	12.657	0.053
17.043	10.693	0.056
13.865	8.781	0.051
10.805	6.879	0.056
7.930	5.137	0.050

Angegeben ist die erweiterte Messunsicherheit, die sich aus der Standardmessunsicherheit durch Multiplikation mit dem Erweiterungsfaktor $k=2$ ergibt. Sie wurde gemäß DAkkS-DKD-3 ermittelt. Der Wert der Messgröße liegt mit einer Wahrscheinlichkeit von 95 % im zugeordneten Wertintervall.

Die Deutsche Akkreditierungsstelle GmbH ist Unterzeichnerin der multilateralen Übereinkommen der European co-operation for Accreditation (EA) und der International Laboratory Accreditation Cooperation (ILAC) zur gegenseitigen Anerkennung der Kalibrierscheine. Die weiteren Unterzeichner innerhalb und außerhalb Europas sind den Internetseiten von EA (www.european-accreditation.org) und ILAC (www.ilac.org) zu entnehmen.

The expanded uncertainty assigned to the measurement results is obtained by multiplying the standard uncertainty by the coverage factor $k = 2$. It has been determined in accordance with DAkkS-DKD-3. The value of the measurand lies within the assigned range of values with a probability of 95%.

The DAkkS is signatory to the multilateral agreements of the European co-operation for Accreditation (EA) and of the International Laboratory Accreditation Cooperation (ILAC) for the mutual recognition of calibration certificates.

1 Detailed Calibration Results

DKD calibration no. 1413414

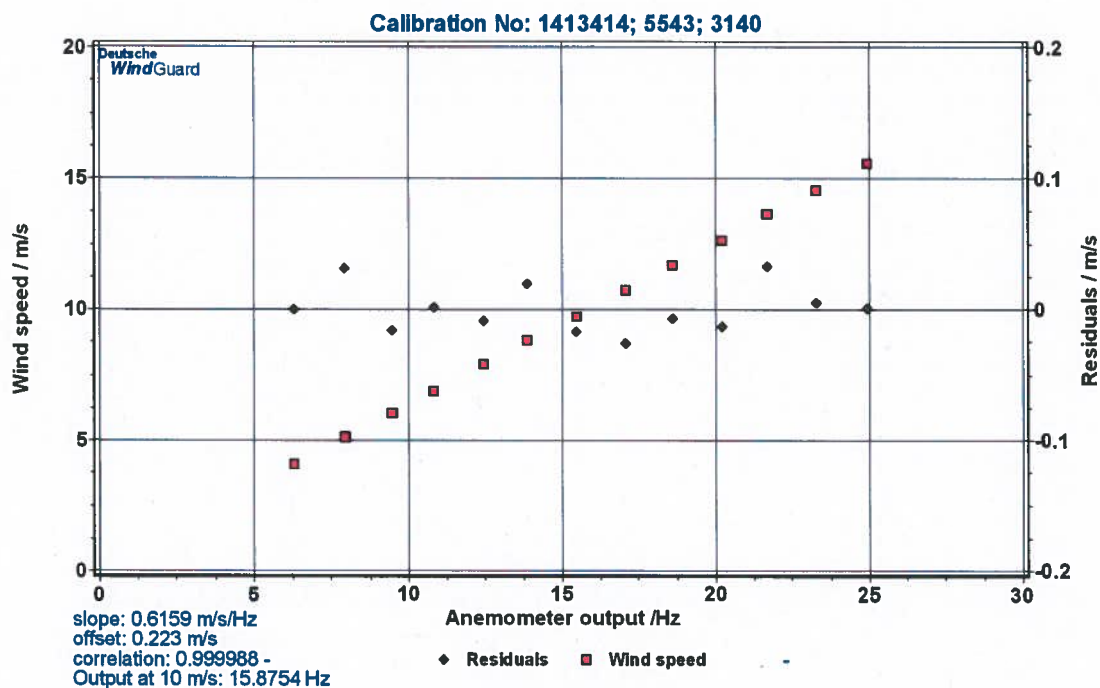
Serial no. 1 5543
Serial no. 2 3140
Date 26.06.2014
Air temperature 22.7 °C
Air pressure 1015.6 hPa
Humidity 46.9 %



Linear regression analysis

Slope $0.61586 \text{ (m/s)/(Hz)} \pm 0.00092 \text{ (m/s)/(Hz)}$
Offset $0.2230 \text{ m/s} \pm 0.015 \text{ m/s}$
St.err(Y) 0.015 m/s
Correlation coefficient 0.999988

Remarks no



Deutsche WindGuard Wind Tunnel Services is accredited by MEASNET and by the Deutsche Akkreditierungsdienst – DAkkS (German Accreditation Service). Registration: D-K-15140-01-00

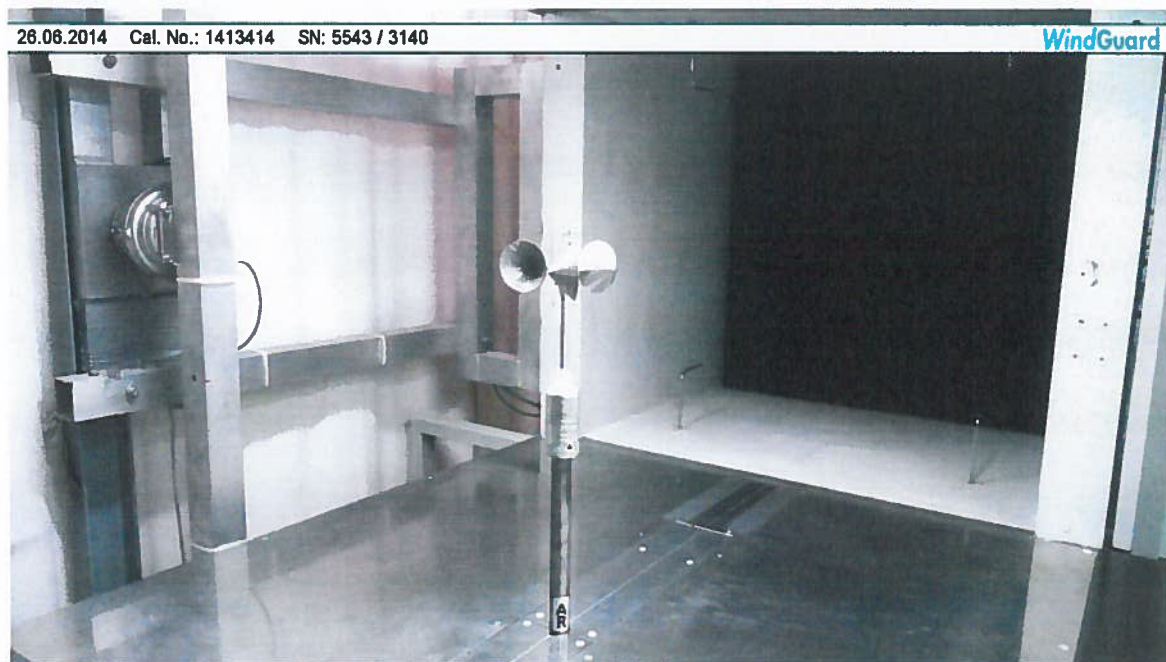
2 Instrumentation

Pos.	Sensor	Manufa.	Type	Range
1	Pitot static tube	Airflow	NPL 8 mm	-
2	Pitot static tube	Airflow	NPL 8 mm	-
3	Pitot static tube	Airflow	NPL 8 mm	-
4	Pitot static tube	Airflow	NPL 8 mm	-
5	Pressure transducer	Setra	C 239	250 Pa
6	Pressure transducer	Setra	C 239	250 Pa
7	Pressure transducer	Setra	C 239	250 Pa
8	Pressure transducer	Setra	C 239	250 Pa
9	El. Barometer	Vaisala	3.11.57.10.000	800hPa -1200 hPa
10	El. Thermometer	Galltec	KPK 1/6-ME	10° C - 40° C
11	El. Humidity sensor	Galltec	KPK 1/6-ME	0-100 %
12	Wind tunnel control	-	-	-
13	CAN-BUS / PC	esd	24 x 16 bit	

Table 1 Description of the data acquisition system

Remark: Last Re-accreditation see page 2

3 Photo of the calibration set-up



Calibration set-up of the anemometer calibration in the wind tunnel of Deutsche WindGuard, Varel. The anemometer shown may differ from the calibrated one. Remark: The proportion of the set-up is not true to scale due to imaging geometry.

4 Deviation to IEC procedure

The calibration procedure is in all aspects in accordance with the IEC 61400-12-1 Procedure

5 References

- [1] D. Westermann, 2009 – Verfahrensanweisung DKD-Kalibrierung von Windgeschwindigkeitssensoren
- [2] IEC 61400-12-1 12/2005 – Power performance measurements of electricity producing wind turbines
- [3] ISO 3966 2008 – Measurement of fluid flow in closed conduits